

An association between past levels of ozone column depletion and the pollen morphology of the model angiosperm *Arabidopsis thaliana* L

Murphy, B.R. and Mitchell, F.J.G.

Review of Palaeobotany and Palynology

Volume 194, 15 July 2013, Pages 12–20

Abstract

The currently reduced stratospheric ozone layer remains sensitive to destructive anthropogenic and natural inputs. We hypothesised that a sudden increase in surface ultraviolet-B (UV-B) irradiation, as may have occurred in a past mass extinction event, would have a significant effect on the pollen grain morphology of the model angiosperm *Arabidopsis thaliana* L. Plants of *A. thaliana* in controlled-environment chambers were exposed to an increase in UV-B irradiation associated with an ozone column reduction of 70%. Pollen grains were examined with light and electron microscopy for morphological abnormalities. In this study, we found that a wild-type *A. thaliana* accession showed a significant increase in the proportion of pollen grain morphological abnormalities in response to the increase in UV-B irradiation. Plants exposed to normal daylight in early growth had less pollen morphological abnormalities when exposed to a subsequent increase in UV-B. Results here suggest that any future decrease in stratospheric ozone similar to that implicated in the end-Permian mass extinction event may increase angiosperm pollen morphological abnormalities, with uncertain and potentially negative consequences for plant reproductive success.

Keywords

- ultraviolet-B irradiation;
- ozone layer;
- pollen abnormalities;
- *Arabidopsis thaliana*;
- mass extinction event

1. Introduction

1.1. Ultraviolet radiation and plants

Plant responses to incident solar radiation are many and varied. While plants may suffer stress from over-exposure to light in the visible wavelength range, radiation in the shorter wavelength and higher energy ultraviolet (UV) range

(40–400 nm) has a greater potential to damage both the tissues and DNA of plants and other organisms (Wong and Parisi, 1996). Fortunately, most of the energy in the UV waveband is absorbed by components of the Earth's atmosphere, especially the stratospheric ozone (O₃) layer (McKenzie et al., 2011).

Recent ozone layer reduction, mostly resulting from human introduction of chlorofluorocarbons (CFCs) into the atmosphere, was first studied in the early 1980s (Farman et al., 1985), stimulating subsequent investigations into the possible effects on Earth's biota. Research regarding the stability of the ozone layer raised concerns about increasing amounts of UV radiation reaching the Earth's surface and causing biological damage (Worrest and Caldwell, 1986, Caldwell et al., 1989 and Qing et al., 2004). Sessile plants have evolved protective mechanisms against ultraviolet radiation and though less sensitive than other macro-organisms to ultraviolet radiative stress (Landry et al., 1995 and Rozema et al., 2001), plant response to stress impacts on many other life-forms. There is a continuing global reduction in the ozone layer compared to the pre-ozone hole period, which may make it particularly vulnerable to any further perturbation (Jackson, 2011).

Plant reproductive capacity is an important determinant in long-term species survival, and the viability of pollen is a crucial element in the reproductive processes of higher plants. Particularly pertinent would be any impact on the production potential of seed-producing crops. The total estimated value of the world market in commercial seeds as of 2008 was \$US36.5 billion (Millstone and Lang, 2008). Atmospheric components other than the ozone layer strongly affect UV-B surface values, for example cloud cover, aerosols and optical depth (Blumthaler and Ambach, 1990 and Nemeth et al., 1996). Nemeth et al. (1996), in a long-term series of studies, found that there was no increase in surface UV-B despite ozone depletion, partly due to the effects of these atmospheric parameters. Despite these confounding factors and because our reference UV-B values have been based on current local measurements, the effects of increased surface UV-B irradiation should accurately reflect the consequences of a local ozone column reduction.

1.2. Research into UV-B effects on plants

Much of the research on the effects of UV-B on plants has focused on changes in plant growth and productivity, gamete viability and genetic changes (Demchik and Day, 1996, Torabinejad et al., 1998, Walbot and Casati, 2004 and Lake et al., 2009). Responses to increased UV-B irradiation vary considerably between plant groups, depending on evolved characteristics and life history (Caldwell et al., 1989, Teramura et al., 1991 and Wolf et al., 2010). The few studies of the effects of increased UV-B irradiation on pollen grains indicate an increase in pollen grain morphological abnormalities (Koti et al., 2004). There are three

compartments in the pollen grain that absorb UV-B: cytoplasmic, pollen wall-bound and the outer sporoderm (Fig. 1), and there is some evidence that UV-B absorbance within the sporopollenin polymer component of the exine increases with enhanced solar UV-B (Rozema et al., 2001). The pollen wall screens out greater than 80% of total UV-B, allowing ~ 20% UV-B to be transmitted into the cytoplasm of the pollen cell (Yeloff et al., 2008). Multiple causes of pollen grain abnormalities have been demonstrated in other studies, mostly due to developmental disorders related to gene malfunctioning (Takahashi, 1989, Ariizumi et al., 2004, Cheng et al., 2004, Morant et al., 2007, Suzuki et al., 2008 and Wilson and Zhang, 2009).

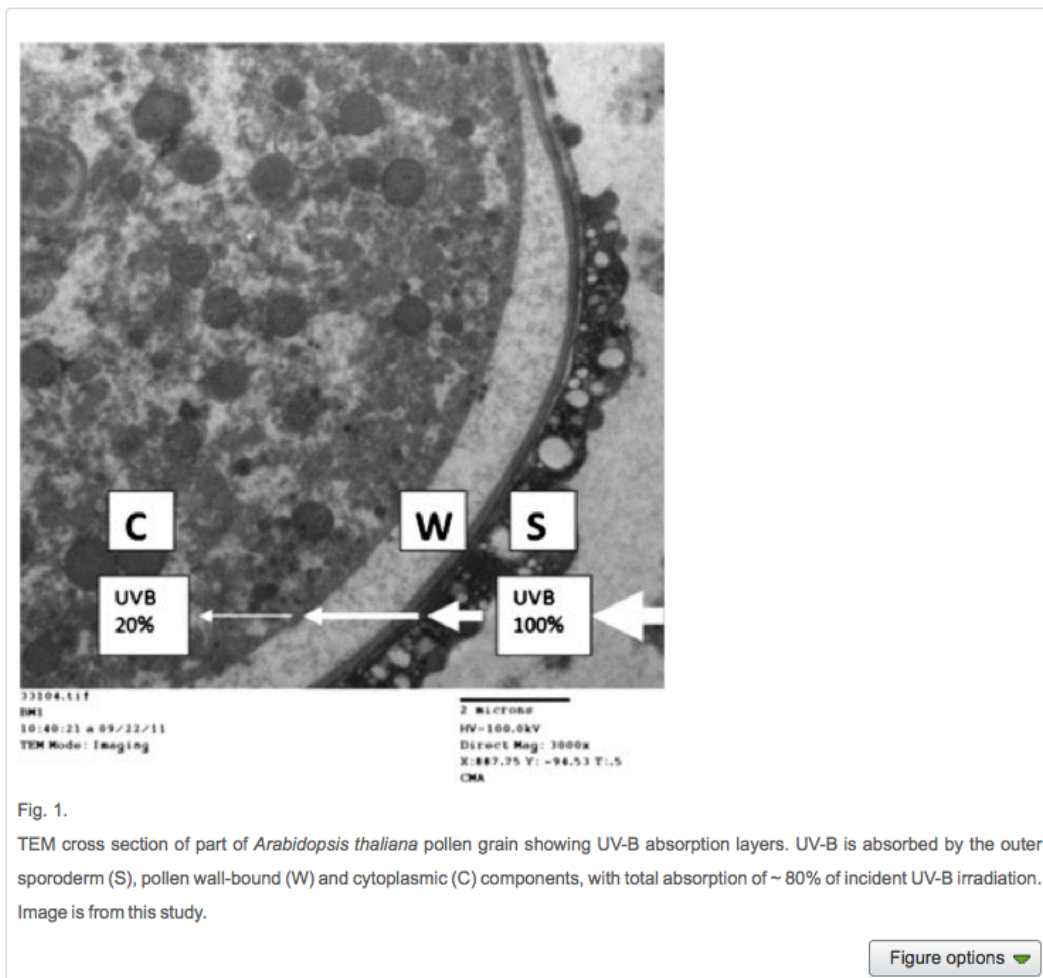


Fig. 1.

TEM cross section of part of *Arabidopsis thaliana* pollen grain showing UV-B absorption layers. UV-B is absorbed by the outer sporoderm (S), pollen wall-bound (W) and cytoplasmic (C) components, with total absorption of ~ 80% of incident UV-B irradiation. Image is from this study.

TEM cross section of part of *Arabidopsis thaliana* pollen grain showing UV-B absorption layers. UV-B is absorbed by the outer sporoderm (S), pollen wall-bound (W) and cytoplasmic (C) components, with total absorption of ~ 80% of incident UV-B irradiation. Image is from this study.

1.3. Past increases in UV-B irradiation

Fluctuations in the amount of UV-B radiation reaching the Earth's surface are not just a modern phenomenon. Various indirect methods have been used to assess surface UV-B in the past (Blokker et al., 2005 and Bjorn and McKenzie, 2007). Studies focussing on fossil pollen have indicated that past atmospheric instability may have caused temporary increases in surface UV-B leading to abnormal pollen grain morphology (Looy et al., 1999, Visscher et al., 2004, Foster and Afonin, 2005, Beerling et al., 2007, Mc Elwain and Punyasena, 2007 and Hochuli et al., 2010). In one study, abnormal fossil gymnosperm pollen morphotypes from the same species were found thousands of kilometres apart in coeval localities in Russia and north-west China, providing independent evidence of deteriorating global atmospheric conditions at the end of the Permian (Foster and Afonin, 2005). Pollen abnormalities were found to be similar to those in extant conifers, caused by atmospheric pollution or increased levels of UV-B. Visscher et al. (2004) documented the widespread occurrence of unseparated fossil lycopsid pollen tetrads at the latest Permian, and they also proposed that prolonged exposure to enhanced UV radiation could account for these morphotypes. Foster and Afonin (2005) proposed that an elevated level of UV-B light irradiation was due to a stratospheric ozone reduction of up to 90%, caused by increased atmospheric halogens and chlorine produced from the explosive nature of the Siberian Traps volcanic eruptions at the end of the Permian (251 million years ago). Model simulations of the release of ozone destroying compounds into the atmosphere during this mass extinction event produced column ozone depletion of 70–85% in the northern hemisphere (Beerling et al., 2007). Ozone depletion to this extent may have taken tens of thousands of years and allowed plants to adapt gradually. For this reason, we recognise that it may be difficult to equate our results with palaeoresponses. Nevertheless, anthropogenic activity may increase the chances of an equivalent sudden ozone reduction. Such a reduction may have serious consequences for food crop production due to a possible negative effect on pollen viability.

Using the estimated ozone column reduction at the end-Permian mass extinction event as a guide, this paper will examine the effects of an increase in UV-B irradiation, associated with a hypothetical ozone column reduction of 70%, on the pollen grain morphology of the model angiosperm *Arabidopsis thaliana* L. wild-type (WT) accession 'Columbia'.

1.4. Experimental plant choice

Arabidopsis thaliana was chosen as the experimental subject for the very same reasons that this plant has become the model angiosperm of choice for plant studies; i.e. small size and simple growing requirements, self-fertilising producing thousands of seeds from a single plant, and a relatively short life-cycle of approximately eight weeks. The morphology of *Arabidopsis* pollen grains has been extensively studied and imaged so there is a degree of confidence associated with the assessment of any observed abnormalities. In the current

study, small or subtle differences in ornamentation, apertural and other patterning were considered to be within the normal range of variability (Van Campo, 1976 and Borsch and Wilde, 2000), and only obvious 'gross' differences were classed as abnormal.

2. Materials and methods

2.1. UV-B dosage estimation

Prior to the application of the treatment dose of UV-B radiation, measurements of local outdoors UV-B flux were made over 28 days (at latitude 53° 25' N between 27th June and 24th July 2011), to supply an accurate reference for subsequent calculations of UV-B dosage. Seven measurements per day were carried out, covering the full daylight period (from 05:30 to 21:30 GMT). A mean value over 120 s was recorded for each measurement. Measurements were made using a Vernier UV-B Sensor (responding to 290–320 nm, with a resolution of 0.25 mW m⁻² and UV peak sensitivity of 1 V per 204 mW m⁻² at 315 nm) and a Vernier Go! Link computer interface. Results were analysed using Vernier Logger Lite 1.5 software running on a MS Windows® compatible PC. For each measurement the UV-B sensor was pointed at the brightest part of the sky visible from where the outdoor experimental plant sets would be grown (see below).

2.2. Plant growth

Four 40-cell seed sowing trays (each cell with a depth of 85 mm and top diameter of 40 mm) were sterilised using Milton® sterilising fluid diluted one part to 20 parts water for 30 min. A seed sowing compost of two parts Forker® John Innes No.1 and one part medium grade moss peat was mixed, and each cell filled with this compost to within 5 mm of the top. Two granules of Osmocote® were added to the top 10 mm of each cell to act as a slow release fertiliser during the growing period. Trays were lightly tapped and watered thoroughly from below, drained, and left covered overnight in black plastic. Four seeds of wild-type *Arabidopsis thaliana* L. accession 'Columbia' were surface-sown into each cell, and the four trays covered in cling-film (to maintain humidity around the seeds until germination) and placed in a refrigerator at 4 °C for 5 days.

After removing the seed trays from the refrigerator the trays were placed in two locations. Two trays were placed outdoors against an east-facing wall and two trays placed in a Conviron Adaptis CMP-6010 growth chamber. Growth chamber environmental settings were programmed for a photoperiod of 16.5 h at 18 °C, with photosynthetically active radiation (PAR) of 210 μmol m⁻² s⁻¹ photon flux density, 7.5 h darkness at 11 °C, and a constant relative humidity of 65%. It is important to note that the growth chamber light spectrum contained no UV-B component. These environmental settings were chosen to simulate outdoor conditions during the growth period. The outdoor position for the two trays was chosen as it was a sheltered site with minimal light and moisture stress. One of

the outdoor sets was subsequently placed in the treatment chamber prior to flower bud formation. This produced an experimental design where the outdoor sets were designated as Outdoor Control (OC) and Outdoor Treatment (OT), and growth chamber sets designated as Growth Chamber Control (GC) and Growth Chamber Treatment (GT). The experimental setup enabled an assessment of any effects related to early exposure to ambient full-spectrum light. Results obtained for the outdoor control set (OC) should reflect normal background responses to ambient UV-B. The control sets (GC and OC) remained in their original position and the treatment sets (GT and OT) were subjected to the treatment UV-B dosage. After seed germination the covering cling-film was removed. Plants were continuously monitored and were kept well-watered, suffering no moisture stress during the growth period. General plant health remained good throughout.

2.3. UV-B treatment application

Treatments affecting pollen grain development need to be given before the early tetrad stage (Takahashi and Skvarla, 1991 and Paxson-Sowders et al., 1997). Before flower bud initiation (14 days after germination), the treatment sets GT and OT were moved into another Conviron Adaptis CMP-6010 growth chamber with the same environmental settings as above. UV-B treatments were applied to the GT and OT sets within this growth chamber using a Corona Mini-Lite 3U narrow-band 311 nm UV-B lamp unit, containing 2 × 36W UV-B lamps (supplied by pbbhealthcare.com). This unit delivers energy only at the UV-B wavelength of 311 nm. A timer was used to switch the unit on and off every 15 min during the photoperiod (16.5 h) in an attempt to somewhat reflect the variable outdoor UV-B flux. UV-B dosage was based on the previously recorded local outdoor readings. A mean constant outdoors UV-B flux during daylight hours of 55.8 mW m⁻² was calculated for the four week UV-B measurement period, and this value was used as a basis for estimating UV-B dosage. The relative increase in biologically effective radiation for a given amount of ozone reduction, the radiation amplification factor (Caldwell et al., 1989), is a 1.55% increase in surface UV-B for every 1% reduction in ozone (Feldheim and Conner, 1996 and Hollosy, 2002). As a hypothetical 70% ozone column reduction was being tested, a continuous dosage value of 116 mW m⁻² at 311 nm was used over the full photo period. To cater for the times (half of the dosage time) when the UV-B lamp would be switched off this value was then doubled. Therefore, the final UV-B dosage value used for the treatment period was 232 mW m² at 311 nm. Treatments were continued until silique splitting and seed release.

2.4. Microscopy

Whole flowers from each experimental set were harvested over a period of one week and placed into sterilised and sealed 5 ml glass tubes for each set. The total number of flowers harvested for each set was between 100 and 150.

For scanning electron microscopy (SEM) and transmission electron microscopy (TEM), flowers were temporarily stored in one part 70% ethanol and one part 0.1 M potassium phosphate buffer (pH 7.0) in sealed glass tubes. Flowers were gently crushed in the tube using a glass rod and the solution passed through an 85 μm nylon sieve to separate out the pollen grains. Approximately 5 ml of 70% ethanol was used to flush through the sieve. The pollen in solution was concentrated into a pellet by centrifuging at 4000 rpm for 3 min.

Pelleted pollen grains were processed for SEM and TEM image analysis by fixing in 3% glutaraldehyde and 0.05 M potassium phosphate buffer (pH 6.8) in corked vials on an agitator for 1.5 h at room temperature, with a secondary fixation in buffered 2% osmium tetroxide (OsO_4) on an agitator for 30 min. The samples were dehydrated using an overnight 10%–100% alcohol series. An alcohol series dehydration was chosen in preference to an acetone series in order to minimise the chances of pollen grain shrinkage. For SEM, dried pollen grains were deposited on a stub and vacuum coated in gold particles. For TEM, samples were prepared for transition to resin by washing in 100% propylene oxide for 45 min with one change of wash solution. For embedding, samples were placed in 50% Agar 100 Epoxy resin for 3 h, changing to a 100% resin mixture for a further 3 h. Samples were transferred to pans with fresh 100% resin and placed in a vacuum to remove air bubbles from the resin. After 2 days the resin embedded pollen grains were sectioned into 70 nm thick slices using diamond and glass microtomes. Thin sections were post-stained by first placing the thin section grid on a drop of 0.5% aqueous uranyl acetate for 30 min, washing with filtered distilled water and drying with Whatman No. 50 filter paper. Grids were further stained by placing on a drop of Reynold's lead citrate stain for 10 min, then washing and drying as above. For SEM images, a Tescan MiraXMU Field Emission Variable Pressure SEM was used, and for TEM images a Jeol JEM2100 operated at 100 kV.

Both fresh pollen and pollen prepared for SEM and TEM were examined in order to achieve a balanced assessment of pollen grain morphology (Hesse and Waha, 1989). For the fresh pollen light microscopy (LM) observations, dehiscent anthers on whole flowers were pressed onto glass microscope slides to deposit the pollen grains onto the slide. LM images were made using an Olympus C-5060 digital camera attached to an Olympus BX60 microscope.

2.5. Pollen grain analysis

For the pollen grain analyses, a series of 10 random locations, approximately 300 \times 300 μm in area, for each set were selected on each SEM stub, TEM thin section or LM slide, and examined for the presence of pollen grain abnormalities. The 9 \times 104 μm^2 grid size chosen for each observation allowed individual pollen grains to be clearly examined whilst also having an adequate number of pollen grains in each grid (*Arabidopsis* pollen grains are \sim 30 μm in length, so there was a

potential for 100 individual pollen grains in each field of view). This grid size choice also meant that over half of the total area on each SEM stub or TEM section was examined. Pollen grains with suspected morphological abnormalities were more closely examined using a higher magnification. Total pollen grain counts were recorded at each location and the percentage of abnormal pollen grains calculated. If a random location contained no pollen grains, then the nearest location to this with grains present was examined.

Pollen grain morphological abnormalities were categorised according to type (collapsed grain, misshapen grain, abnormal aperture, pollen wall abnormalities and undeveloped grain). Small differences in pollen grain size were not classed as abnormalities, as these differences in size are to be expected as normal variation (Van Campo, 1976 and Khan, 2004).

At each of the ten random locations chosen for pollen grain examination in the LM and SEM preparations, the dimensions (equatorial diameter and polar axis length) of two normal pollen grains were measured. The pollen grain dimensions in the TEM preparations could not be accurately determined.

As a follow-up estimation of seed viability, ~ 100 seeds that were produced from each set were sown into 90 mm plastic pots in the same compost as the initial sowing. This was done in early September with fresh seeds harvested from each experimental set. As before, pots were covered in cling film to maintain humidity around the seeds. All pots were placed outside in an east-facing location, and germination monitored.

3. Results

Pollen grain morphological abnormalities were detected under the three different observation techniques (SEM, TEM and LM). The abnormalities were relatively easy to determine in the SEM images, where details of pollen grain surface morphology could be closely examined (Fig. 2). Some debris and bacteria were observed on the SEM images due to unavoidable contamination during harvesting and short-term storage (Fig. 2), but the quality of most images was acceptable. An example of different developmental fates for individual pollen grains after mother-cell meiosis was seen in a group of three attached pollen grains (probably members of a single tetrad) which contained one normal grain, a misshapen grain and an undeveloped grain (Fig. 3).

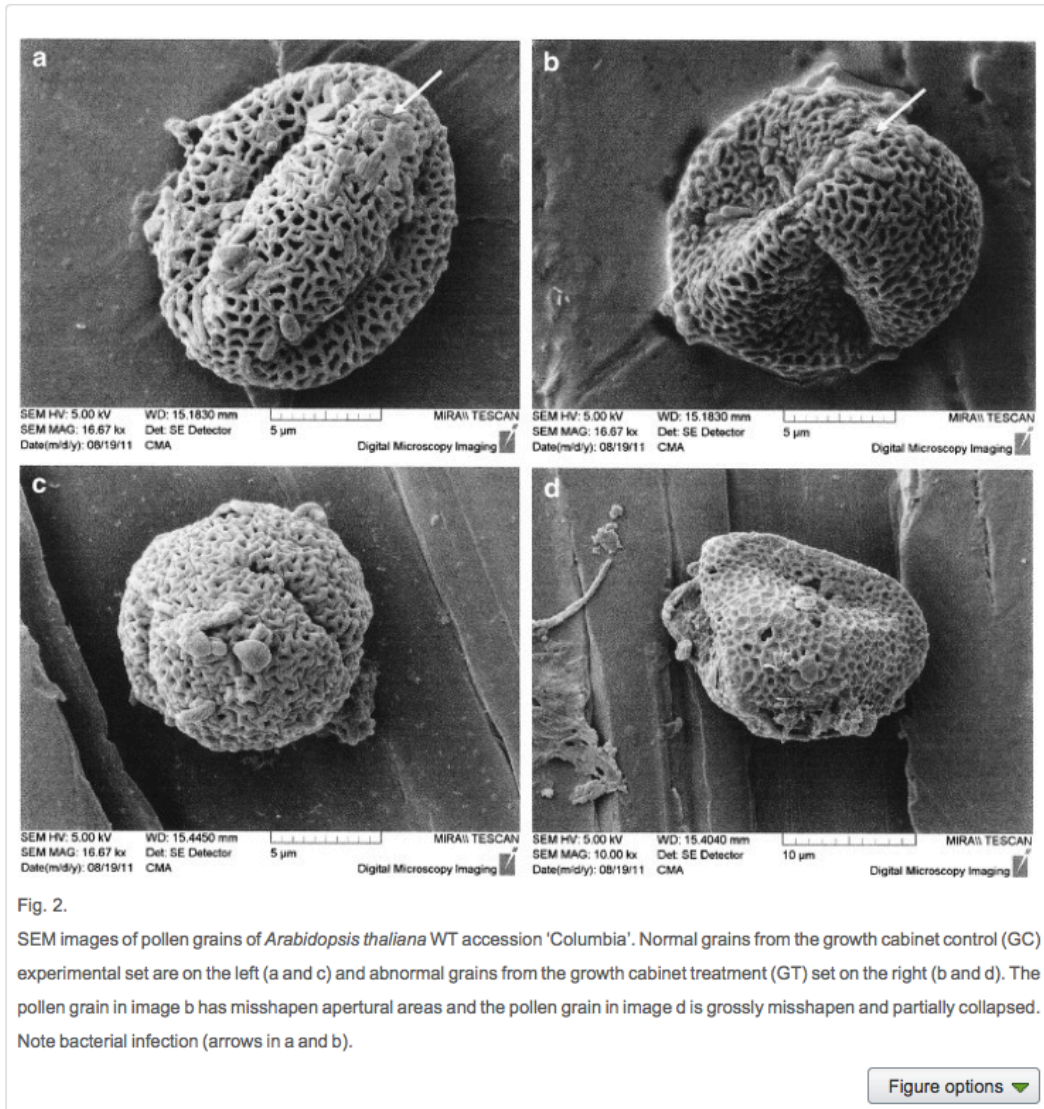


Fig. 2.

SEM images of pollen grains of *Arabidopsis thaliana* WT accession 'Columbia'. Normal grains from the growth cabinet control (GC) experimental set are on the left (a and c) and abnormal grains from the growth cabinet treatment (GT) set on the right (b and d). The pollen grain in image b has misshapen apertural areas and the pollen grain in image d is grossly misshapen and partially collapsed. Note bacterial infection (arrows in a and b).

Figure options ▼

Fig. 2.

SEM images of pollen grains of *Arabidopsis thaliana* WT accession 'Columbia'. Normal grains from the growth cabinet control (GC) experimental set are on the left (a and c) and abnormal grains from the growth cabinet treatment (GT) set on the right (b and d). The pollen grain in image b has misshapen apertural areas and the pollen grain in image d is grossly misshapen and partially collapsed. Note bacterial infection (arrows in a and b).

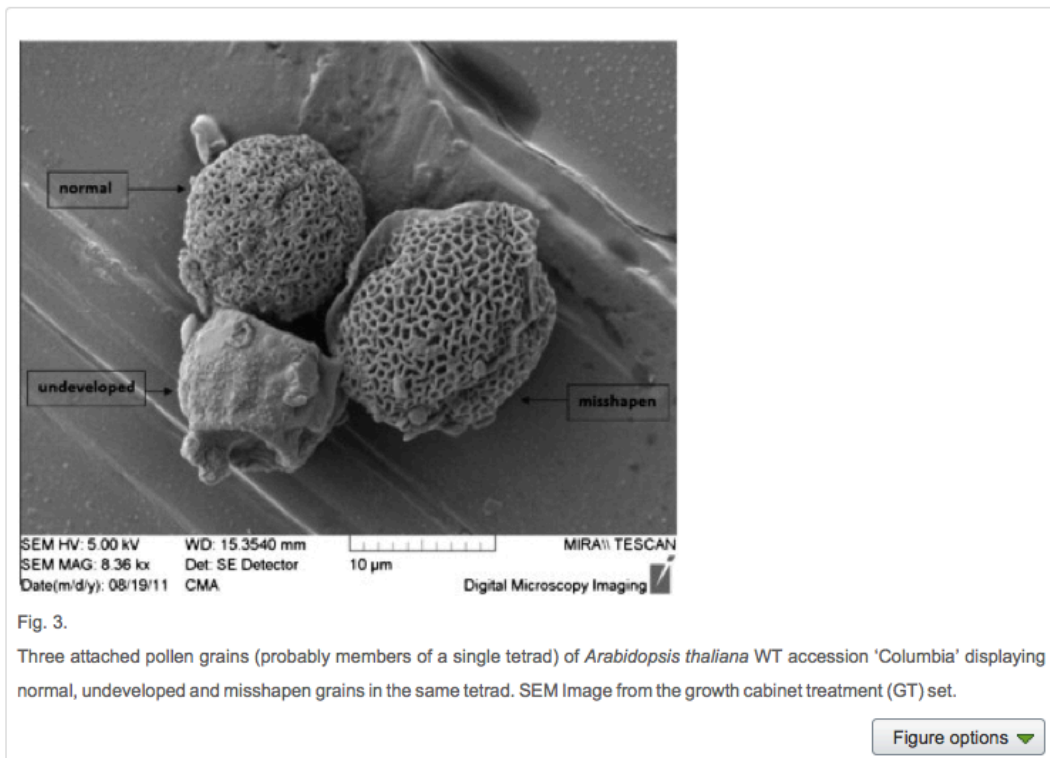


Fig. 3.

Three attached pollen grains (probably members of a single tetrad) of *Arabidopsis thaliana* WT accession 'Columbia' displaying normal, undeveloped and misshapen grains in the same tetrad. SEM Image from the growth cabinet treatment (GT) set.

TEM sections revealed a range of pollen wall abnormalities, including shrunken cytoplasmic compartments, misshapen grains, malformed endexine and foot layers, and gaps in the ectexine (Fig. 4). Close-ups of the pollen wall of some grains showed immature foot, endexine and intine layers (Fig. 4c) which are normally associated with developing grain architecture prior to tetrad splitting (Harley et al., 2000).

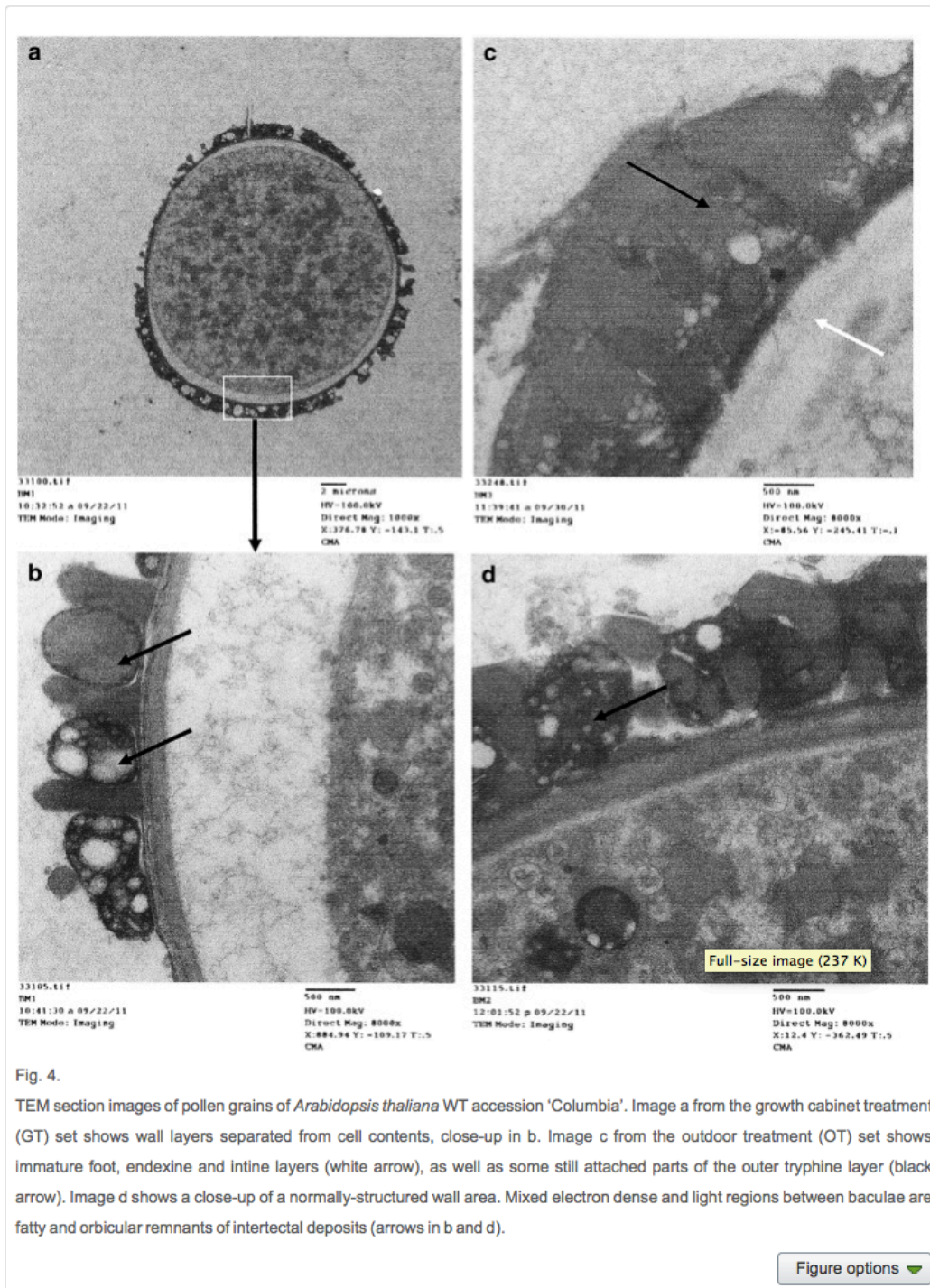


Fig. 4.

TEM section images of pollen grains of *Arabidopsis thaliana* WT accession 'Columbia'. Image a from the growth cabinet treatment (GT) set shows wall layers separated from cell contents, close-up in b. Image c from the outdoor treatment (OT) set shows immature foot, endexine and intine layers (white arrow), as well as some still attached parts of the outer tryphine layer (black arrow). Image d shows a close-up of a normally-structured wall area. Mixed electron dense and light regions between baculae are fatty and orbicular remnants of intertectal deposits (arrows in b and d).

electron dense and light regions between baculae are fatty and orbicular remnants of intertectal deposits (arrows in b and d).

Low resolution light microscope (LM) images revealed less detail than the SEM and TEM images, but nevertheless demonstrated some clear examples of pollen grain abnormality (Fig. 5). It was difficult to confidently equate types of abnormality in the LM, SEM and TEM images, particularly as the overlying tryphine and superficial layers in the fresh pollen (LM) obscured details of grain ornamentation and patterning. Nevertheless some of the images from the different preparations could be matched in terms of abnormality class (Fig. 6).

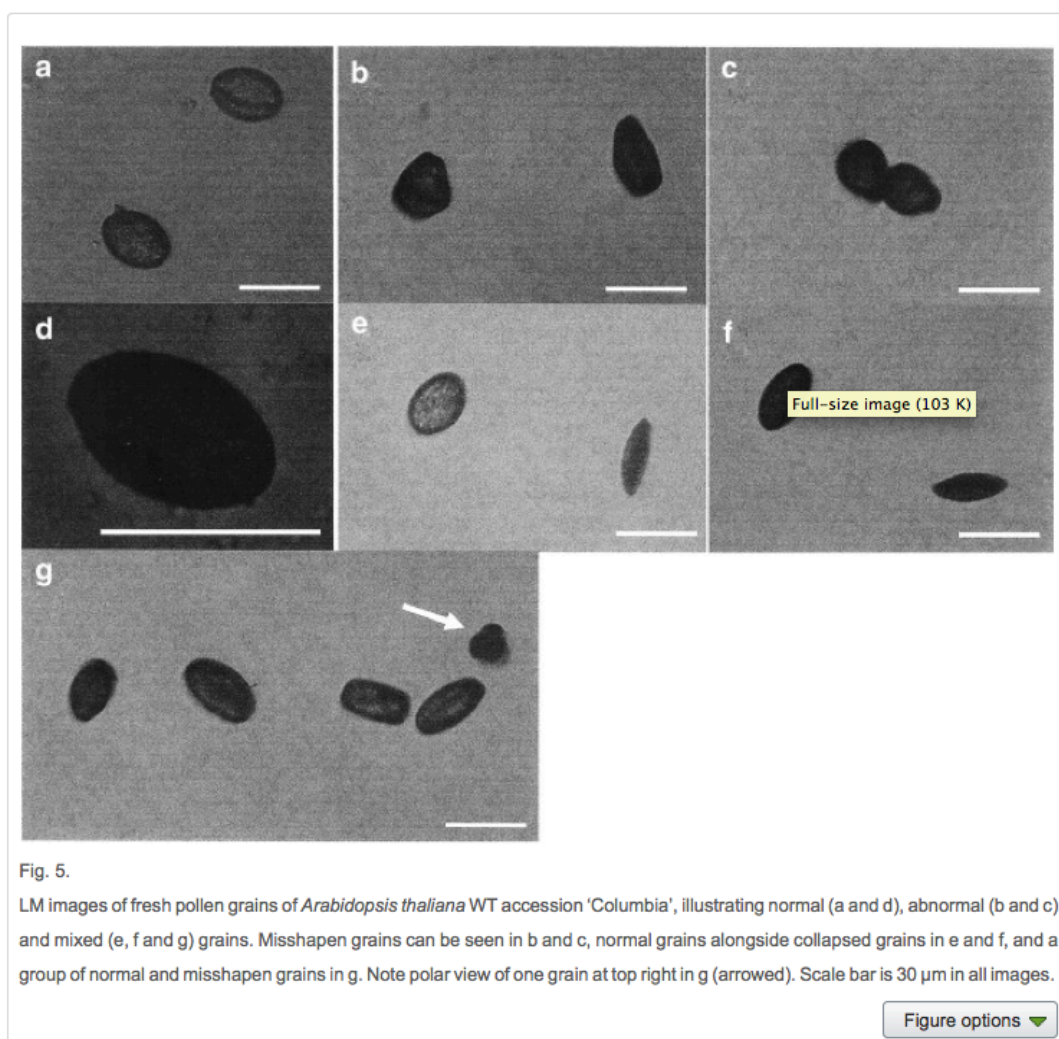


Fig. 5.

LM images of fresh pollen grains of *Arabidopsis thaliana* WT accession 'Columbia', illustrating normal (a and d), abnormal (b and c) and mixed (e, f and g) grains. Misshapen grains can be seen in b and c, normal grains alongside

collapsed grains in e and f, and a group of normal and misshapen grains in g. Note polar view of one grain at top right in g (arrowed). Scale bar is 30 μm in all images.

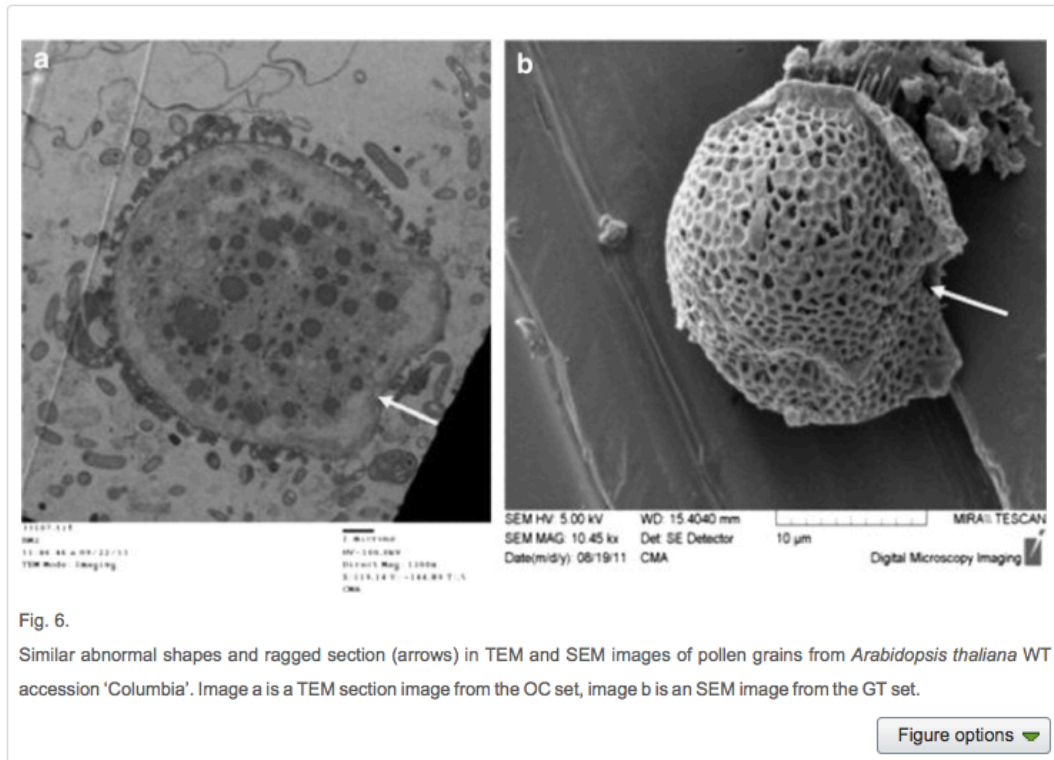


Fig. 6.

Similar abnormal shapes and ragged section (arrows) in TEM and SEM images of pollen grains from *Arabidopsis thaliana* WT accession 'Columbia'. Image a is a TEM section image from the OC set, image b is an SEM image from the GT set.

Figure options


There were 84 pollen grain abnormalities found in 565 pollen grain observations in the combined SEM, TEM and LM preparations for all experimental sets. The mean percentage of abnormalities found was 3.2 times greater in the combined treatment sets (7.7%) than in the combined control sets (2.4%) (Table 1).

Table 1.

Number of pollen grains examined and percentage of observed pollen grain abnormalities in *Arabidopsis thaliana* WT accession 'Columbia', showing relationship to increasing UV-B dosage. UV-B increase from initial to treatment

dosage shown for OT and GT sets. Data are from 10 randomly examined locations in each experimental set of the SEM, TEM and LM preparations.

Table 1.
Number of pollen grains examined and percentage of observed pollen grain abnormalities in *Arabidopsis thaliana* WT accession 'Columbia', showing relationship to increasing UV-B dosage. UV-B increase from initial to treatment dosage shown for OT and GT sets. Data are from 10 randomly examined locations in each experimental set of the SEM, TEM and LM preparations.

Increasing UV-B dosage 

Treatment	GC	OC	OT	GT
UV-B dosage (mW m ⁻²)	0	59	59 >> 232	0 >> 232
SEM % abnormalities	1.7	2.5	5.2	9.7
TEM % abnormalities	2.3	2.5	7	6.5
LM % abnormalities	2.9	2.5	8.7	9
No. grains examined	174	121	115	155
Mean % abnormalities	2.3	2.5	7	8.4

Table options ▼

An analysis of pollen grain abnormality categories showed that misshapen grains were the most common type of abnormality (38%), with pollen grain wall abnormalities (29%) the next most frequent category (note that this category was restricted to the TEM preparations). Almost half of the abnormalities (49%) were found in the GT set, and the combined treatment sets (GT and OT) accounted for 77% of abnormalities found (Table 2).

Table 2.

Pollen grain abnormalities by percentage (of 84 abnormalities) in each abnormality category for 10 random locations observed in *Arabidopsis thaliana* WT accession 'Columbia' from each experimental set for combined SEM, TEM and LM observations, showing relationship to increasing UV-B dosage. UV-B increase from initial to treatment dosage shown for OT and GT sets.

Table 2.

Pollen grain abnormalities by percentage (of 84 abnormalities) in each abnormality category for 10 random locations observed in *Arabidopsis thaliana* WT accession 'Columbia' from each experimental set for combined SEM, TEM and LM observations, showing relationship to increasing UV-B dosage. UV-B increase from initial to treatment dosage shown for OT and GT sets.

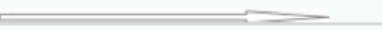
Increasing UV-B dosage 					
Treatment	GC	OC	OT	GT	
UV-B dosage (mW m ⁻²)	0	59	59 » 232	0 » 232	% of total
<i>Pollen abnormality category</i>					
Collapsed	3.6	2.4	6	11.9	23.9
Misshapen	1.2	3.6	10.7	22.6	38.1
Aperture	0	0	2.4	1.2	3.6
Undeveloped	2.4	1.2	0	2.4	6
Pollen wall	4.8	3.6	9.5	10.7	28.6
% of total	12.0	10.8	28.6	48.8	

Table options ▼

A significant linear relationship (regression analysis: $F_{3,27} = 5.63$, $r^2 = 0.9463$, $P < 0.05$) was found between the UV-B dosage and the mean percentage of pollen grain abnormalities observed (Fig. 7). The experimental set which experienced the greatest relative increase in UV-B irradiation (the GT set) had the greatest percentage of pollen grain abnormalities.

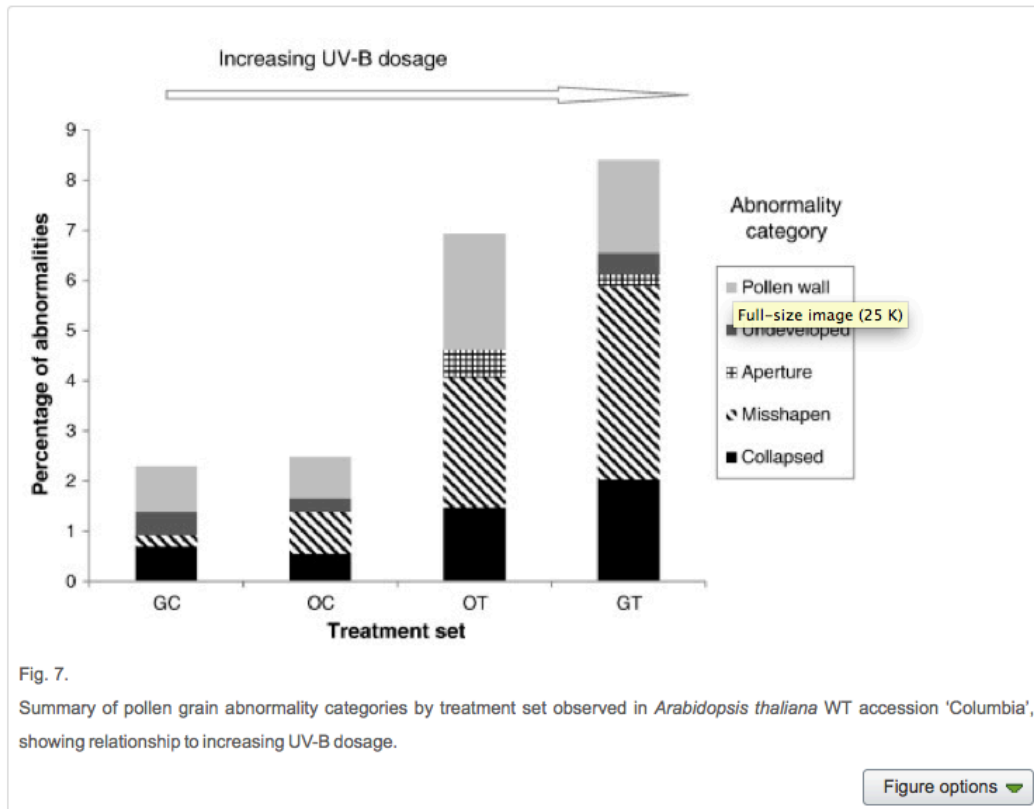


Fig. 7.

Summary of pollen grain abnormality categories by treatment set observed in *Arabidopsis thaliana* WT accession 'Columbia', showing relationship to increasing UV-B dosage.

Figure options

There was a significant difference between the OC (control) and OT (treatment) sets (chi-square test, $\chi^2 = 20.2$, $df = 1$, $P < 0.001$) and between the GC (control) and GT (treatment) sets (chi-square test, $\chi^2 = 64.8$, $df = 1$, $P < 0.001$) in the number of pollen abnormalities expected (the controls) and the number of pollen abnormalities observed (the treatments). In both cases the treatment sets had a significantly greater proportion of pollen abnormalities.

There was no significant correlation (regression analysis; $F_{1,5} = 0.0207$, $r^2 = 0.4\%$, $P > 0.1$) between UV-B dosage (or vegetative to flowering phase UV-B increase) and normal pollen grain size.

From the seeds sown for each set at the end of the experimental period, germination success from ~ 100 seeds sown was 100% for the GT, OC and OT

sets, with the GC set (the only experimental set not to have received any UV-B irradiation) having a 58% germination rate.

4. Discussion

4.1. Justifications and interpretation

The analysis of the effects of increased UV-B on pollen grain morphology in this experiment is based on the assessment of abnormalities. Throughout the angiosperms there is significant infraspecific pollen variation resulting from random events during self-assembly processes (Borsch and Wilde, 2000), variation occurring within individuals and even within single pollen sacs (Van Campo, 1976). It was therefore important to know exactly what kinds of pollen abnormalities to look for, as subtle pollen grain differences may be a result of natural variation.

The placing of pollen grain abnormalities into a single category is a subjective exercise, with some grains falling into more than one category (e.g. collapsed and also misshapen). Different quantities of UV-B irradiation may produce different abnormalities, and a large ratio of misshapen and collapsed grains, as found in our study, have been shown to be associated with the particular experimental UV-B dosage used (Koti et al., 2004). Further, the type of abnormality may be related to other causes, and there will always be a background level of abnormalities regardless of any treatments applied (as shown in the outdoor control set).

The increase in UV-B irradiation associated with a 70% decrease in the ozone column has been shown to have a significant effect on the pollen morphology of *Arabidopsis thaliana* WT accession 'Columbia'. The UV-B dosage given in our treatments was only at a narrowband 311 nm wavelength and plant responses have been shown to be varied in comparisons between narrowband and broadband UV-B treatments (Wolf et al., 2010).

The proportion of pollen abnormalities in the experimental sets was directly related to total UV-B dosage. Foster and Afonin (2005) suggest a benchmark of 3% (or greater) abnormality of pollen morphotypes as an indicator of environmental stress. The proportion of pollen abnormalities in our treatment sets was above this threshold, and below this threshold in the control sets.

The GC set, which received no UV-B irradiation throughout plant lifetime, had a similar percentage of abnormalities as the outdoors control (OC). This may be due to a natural background rate of abnormalities regardless of UV-B dosage (Wang et al., 2011), or it may be related to other stress factors. The outdoors

conditioned OT set had less pollen abnormalities than the GT set even though both sets were exposed to the same UV-B dosage during the pollen production phase. As the OT set was initially grown outdoors then a case may be made for an early pre-pollen production protective mechanism induced by ambient full-spectrum light exposure. There is some evidence in the literature that UV-conditioned plants are less stressed by any subsequent increase in UV-B (Hectors et al., 2007).

Conner and Neumeier (2002) showed that offspring derived indirect beneficial effects from enhanced UV-B exposure in parents. This indirect beneficial effect was also seen in the current study, where the experimental set that received no UV-B throughout plant lifetime had a lower seed germination success than all the others. The low proportion of seed germination for the GC set suggests that there may be a positive relationship between a certain degree of UV-B exposure and seed viability. This may also suggest that more unviable seeds survived to maturity than those subjected to the greater selective stress of UV-B exposure. Poor summers with relatively low UV-B exposure have been shown to be associated with a subsequent poor seed set (Rawson et al., 1984). Demchik and Day (1996), using another member of the Brassicaceae (*Brassica rapa*), found that seed abortion rates were higher in plants pollinated with pollen from enhanced UV-B treatments even though seed yield per plant was similar.

The atypical midsummer overcast skies during the UV-B reference measurements resulted in an unrepresentative calculation of the correct UV-B dosage to use as treatment, and a longer term monitoring of outdoor surface UV-B flux at this location would produce a more accurate reference value. The intermittent UV-B treatments used in this study compensated for the lack of natural variation in UV-B flux which is experienced by plants grown outdoors and avoided the problems and stresses related to constant artificial supplemental UV-B (Teramura et al., 1991). More sophisticated treatment setups which offer a finer control of UV-B irradiation may go some way to addressing these issues (McLeod, 1997).

4.2. Limitations and further research

A lab-based experiment will never adequately address or accommodate all the factors involved in a more realistic field-based experiment (UV-B flux variability, temperature, moisture and light fluctuations, edaphic factors and the many other biotic and abiotic influences within an integrated ecosystem are important contributory variables in plant responses). The challenge here is to scale responses determined in the lab to the responses of plants in the field (Wong and Parisi, 1996 and Caldwell and Flint, 1997). As has been partly demonstrated in our study, plants initially grown in a full-spectrum solar irradiance (the OT set) are much less sensitive to a subsequent increase in UV-B (Caldwell et al., 1989 and Teramura et al., 1991).

There is scope for further investigations that may provide more clarity and a greater level of precision in determining whole-plant responses to increased UV-B. The ultimate test in any measurement of reproductive output is the number of viable seeds produced, and results here suggest that there may be a positive role for UV-B conditioning in achieving full viability. Further multi-generational growth chamber-based tests could determine if this is the case; and whether pollen or seed defects are more closely related to lower viable seed set. Productive areas to explore during such an experiment would involve measuring pollen tube germination and tube growth, fertilisation success, the viability of morphologically abnormal pollen grains, and the degree of redundancy in the number of compensatory pollen grains required to achieve full seed set.

Despite widespread public perception to the contrary, ozone column reduction is ongoing, and the stratospheric ozone component remains sensitive to anthropogenic and natural inputs. Though the current ecological relevance of the data may seem to be limited, ozone column depletion due to destructive global events can never be ruled out. Quantifying responses of plants to any UV-B irradiation increase is crucial to understanding the consequences of any future catastrophic ozone loss.

Acknowledgements

Botanical Laboratory Staff at Trinity College Dublin provided essential lab facilities, technical support, material and supplies. Neal Leddy of the Centre for Microscopy and Analysis at Trinity College Dublin provided electron microscopy expertise and advice.

References

Ariizumi et al., 2004

T. Ariizumi, K. Hatakeyama, K. Hinata, R. Inutsugi, I. Nishida, S. Sato, T. Kato, S. Tabata, K. Toriyama

Disruption of the novel plant protein NEF1 affects lipid accumulation in the plastids of the tapetum and exine formation of pollen, resulting in male sterility in *Arabidopsis thaliana*

The Plant Journal, 39 (2004), pp. 170–181

Beerling et al., 2007

D.J. Beerling, M. Horfoot, B. Lomax, J.A. Pyle

The stability of the stratospheric ozone layer during the end-Permian eruption of the Siberian Traps

Philosophical Transactions of the Royal Society, 365 (2007), pp. 1843–1866

Bjorn and McKenzie, 2007

L.O. Bjorn, R.L. McKenzie

Attempts to probe the ozone layer and the ultraviolet-B levels of the past

Ambio, 36 (5) (2007), pp. 366–371

Blokker et al., 2005

P. Blokker, D. Yeloff, P. Boelen, R.A. Broekman, J. Rozema

Development of a proxy for past surface UV-B irradiation: a thermally assisted hydrolysis and methylation py-GC/MS method for the analysis of pollen and spores

Analytical Chemistry, 77 (18) (2005), pp. 6026–6031

Blumthaler and Ambach, 1990

M. Blumthaler, W. Ambach

Indication of increasing solar Ultraviolet-B radiation flux in alpine regions

Science, 248 (1990), pp. 206–208

Borsch and Wilde, 2000

T. Borsch, V. Wilde

Pollen variability within species, populations, and individuals, with particular reference to *Nelumbo*

M.M. Harley, C.M. Morton, S. Blackmore (Eds.), *Pollen and Spores, Morphology and Biology*, The Board of Trustees of the Royal Botanic Gardens, Kew, London (2000)

Caldwell and Flint, 1997

M.M. Caldwell, S.D. Flint

Uses of biological spectral weighting functions and the need of scaling for the ozone reduction problem

Plant Ecology, 128 (1997), pp. 67–76

Caldwell et al., 1989

M.M. Caldwell, A.H. Teramura, M. Tevini

The changing solar ultraviolet climate and the ecological consequences for higher plants

Tree, 4 (12) (1989), pp. 363–367

Cheng et al., 2004

H. Cheng, L. Qin, S. Lee, X. Fu, D.E. Richards, D. Cao, D. Luo, N.P. Harberd, J. Peng

Gibberellin regulates Arabidopsis floral development via suppression of DELLA protein function

Development, 131 (2004), pp. 1055–1064

Conner and Neumeier, 2002

J.K. Conner, R. Neumeier

The effects of ultraviolet-B radiation and intraspecific competition on growth, pollination success, and lifetime female fitness in *Phacelia campanularia* and *P. purshii* (Hydrophyllaceae)

American Journal of Botany, 89 (1) (2002), pp. 103–110

Demchik and Day, 1996

S.M. Demchik, T.A. Day

Effect of enhanced UV-B radiation on pollen quantity, quality, and seed yield in *Brassica rapa* (Brassicaceae)

American Journal of Botany, 83 (5) (1996), pp. 573–579

Farman et al., 1985

J.C. Farman, B.G. Gardiner, J.D. Shanklin

Large losses of total ozone in Antarctica reveal seasonal CO_x/NO_x interaction

Nature, 315 (1985), pp. 207–210

Feldheim and Conner, 1996

K. Feldheim, J.K. Conner

The effects of increased UV-B radiation on growth, pollination success, and lifetime female fitness in two *Brassica* species

Oecologia, 106 (1996), pp. 284–297

Foster and Afonin, 2005

C.B. Foster, S.A. Afonin

Abnormal pollen grains, an outcome of deteriorating atmospheric conditions around the Permian–Triassic boundary

Journal of the Geological Society of London, 162 (2005), pp. 653–659

Harley et al., 2000

M.M. Harley, C.M. Morton, S. Blackmore (Eds.), Pollen and Spores, Morphology and Biology, Royal Botanic Gardens Kew, London (2000)

Hectors et al., 2007

K. Hectors, E. Prinsen, W. De Coen, M.A.K. Jansen, Y. Guisez

Arabidopsis thaliana plants acclimated to low dose rates of ultraviolet B radiation show specific changes in morphology and gene expression in the absence of stress symptoms

New Phytologist, 175 (2007), pp. 255–270

Hesse and Waha, 1989

M. Hesse, M. Waha

A new look at the acetolysis method

Plant Systematics and Evolution, 163 (1989), pp. 147–152

Hochuli et al., 2010

P.A. Hochuli, J.O. Vigran, E. Hermann, H. Bucher

Multiple climatic changes around the Permian–Triassic boundary event revealed by an expanded palynological record from mid-Norway

Geological Society of America Bulletin, 122 (5/6) (2010), pp. 884–896

Hollosoy, 2002

F. Hollosoy

Effects of ultraviolet radiation on plant cells

Micron, 33 (2002), pp. 179–197

Jackson, 2011

L.P. Jackson

Current State of the Ozone Layer

USEPA web site, United States Environmental Protection Agency (2011)
(<http://www.epa.gov/ozone/science/currentstate.html>)

Khan, 2004

R. Khan

Studies on the pollen morphology of the genus *Arabidopsis* (Brassicaceae) from Pakistan

Pakistan Journal of Botany, 36 (2) (2004), pp. 229–234

Koti et al., 2004

S. Koti, K.R. Reddy, V.G. Kakani, D. Zhao, V.R. Reddy

Soybean (*Glycine max*) pollen germination characteristics, flower and pollen morphology in response to enhanced Ultraviolet-B radiation

Annals of Botany, 94 (2004), pp. 855–864

Lake et al., 2009

J.A. Lake, K.J. Field, M.P. Davey, D.J. Beerling, B.H. Lomax

Metabolomic and physiological responses reveal multi-phasic acclimation of *Arabidopsis thaliana* to chronic UV radiation

Plant, Cell & Environment, 32 (2009), pp. 1377–1389

Landry et al., 1995

L.G. Landry, C.C.S. Chapple, R.C. Last

Arabidopsis mutants lacking phenolic sunscreens exhibit enhanced Ultraviolet B injury and oxidative damage

Plant Physiology, 109 (1995), pp. 1159–1166

Looy et al., 1999

C.V. Looy, W.A. Brugman, D.C. Dilcher, H. Visscher

The delayed resurgence of equatorial forests after the Permian–Triassic ecologic crisis

Proceedings of the National Academy of Sciences of the United States of America, 96 (24) (1999), pp. 13857–13862

Mc Elwain and Punyasena, 2007

J.C. Mc Elwain, S.W. Punyasena

Mass extinction events and the plant fossil record

Trends in Ecology & Evolution, 22 (10) (2007), pp. 548–557

McKenzie et al., 2011

R.L. McKenzie, P.J. Aucamp, A.F. Bais, L.O. Bjorn, M. Ilyas, S. Madronich

Ozone depletion and climate change, impacts on UV radiation

Photochemical and Photobiological Sciences, 10 (2011), pp. 182–198

McLeod, 1997

A.R. McLeod

Outdoor supplementation systems for studies of the effects of UV-B radiation

Plant Ecology, 128 (1997), pp. 79–92

Millstone and Lang, 2008

E. Millstone, T. Lang

Atlas of Food

University of California Press, Los Angeles (2008)

Morant et al., 2007

M. Morant, K. Jorgensen, H. Schaller, F. Pinot, B. Lindberg Moller, D. Werck-Reichhart, S. Bak

CYP703 is an ancient cytochrome P450 in land plants catalyzing in-chain hydroxylation of lauric acid to provide building blocks for sporopollenin synthesis in pollen

The Plant Cell, 19 (2007), pp. 1473–1487

Nemeth et al., 1996

P. Nemeth, Z. Toth, Z. Nagy

Effect of weather conditions on UV-B radiation reaching the earth's surface

Journal of Photochemistry and Photobiology B, Biology, 32 (1996), pp. 177–181

Paxson-Sowders et al., 1997

D.M. Paxson-Sowders, H.A. Owen, C.A. Makaroff

A comparative ultrastructural analysis of exine pattern development in wild-type Arabidopsis and a mutant defective in pattern formation

Protoplasma, 198 (1997), pp. 53–65

Qing et al., 2004

L. Qing, T.V. Callaghan, Z. Yuanyuan

Effects of elevated solar UV-B radiation from ozone depletion on terrestrial ecosystems

Journal of Mountain Science, 1 (3) (2004), pp. 276–288

Rawson et al., 1984

H.M. Rawson, R.L. Dunstone, M.J. Long, J.E. Begg

Canopy development, light interception and seed production in sunflower as influenced by temperature and radiation

Australian Journal of Plant Physiology, 11 (4) (1984), pp. 255–265

Rozema et al., 2001

J. Rozema, A.J. Noordijk, R.A. Broekman, A. van Beem, B.M. Meijkamp, N.V.J. de Bakker, J.W.M. van de Staaij, M. Stroetenga, S.J.P. Bohncke, M. Konert, S. Kars, H. Peat, R.I.L. Smith, P. Convey

(Poly)phenolic compounds in pollen and spores of Antarctic plants as indicators of solar UV-B

Plant Ecology, 154 (2001), pp. 11–26

Suzuki et al., 2008

T. Suzuki, K. Masaoka, M. Nishi, K. Nakamura, S. Ishiguro

Identification of kanaoshi mutants showing abnormal pollen exine in *Arabidopsis thaliana*

Plant & Cell Physiology, 49 (10) (2008), pp. 1465–1477

Takahashi, 1989

M. Takahashi

Pattern determination of the exine in *Caesalpinia japonica* (Leguminosae, Caesalpinoideae)

American Journal of Botany, 76 (11) (1989), pp. 1615–1626

Takahashi and Skvarla, 1991

M. Takahashi, J.J. Skvarla

Exine pattern formation by plasma membrane in *Bouganvillea spectabilis* Willd. (Nyctaginaceae)

American Journal of Botany, 78 (8) (1991), pp. 1063–1069

Teramura et al., 1991

A.H. Teramura, M. Tevini, J.F. Bornman, M.M. Caldwell, G. Kulandaivelu, L.O. Bjorn

Terrestrial plants

Chapter 3 Environmental Effects of Ozone Depletion, 1991 Update, United Nations Environment Programme, Nairobi (1991)

Torabinejad et al., 1998

J. Torabinejad, M.M. Caldwell, S.D. Flint, S. Durham

Susceptibility of pollen to UV-B radiation: an assay of 34 taxa

American Journal of Botany, 85 (3) (1998), pp. 360–369

Van Campo, 1976

M. Van Campo

Patterns of pollen morphological variation within taxa

I.K. Ferguson, J. Muller (Eds.), The Evolutionary Significance of the Exine, Academic Press, London (1976), pp. 125–137

Visscher et al., 2004

H. Visscher, C.V. Looy, M.E. Collinson, H. Brinkhuis, J.H. Van Konijnenburg-van Cittert, W.M. Kürschner, M. Sephton

Environmental mutagenesis during the end-Permian ecological crisis

Proceedings of the National Academy of Sciences of the United States of America, 101 (2004), pp. 12952–12956

Walbot and Casati, 2004

V. Walbot, P. Casati

Impact of UV-B radiation on corn (*Zea mays* L.)

Energy Research at Stanford University, US Department of Agriculture, Stanford (2004)

Wang et al., 2011

X. Wang, L. Chen, G. Feng, J. Zhang, L. Huang, S. Zhang, L. Jin

Screening for natural male sterile mutants in alfalfa (*Medicago sativa* L.) varieties

Australian Journal of Crop Science, 5 (12) (2011), pp. 1603–1609

Wilson and Zhang, 2009

Z.A. Wilson, D.-B. Zhang

From Arabidopsis to rice, pathways in pollen development

Journal of Experimental Botany, 60 (5) (2009), pp. 1479–1492

Wolf et al., 2010

L. Wolf, L. Rizzini, R. Stracke, R. Ulm, S.A. Rensina

The molecular and physiological responses of *Physcomitrella patens* to Ultraviolet-B radiation

Plant Physiology, 153 (2010), pp. 1123–1134

Wong and Parisi, 1996

J.C.F. Wong, A.V. Parisi

Assessment of ultraviolet radiation exposures in photobiological experiments

School of Physical Sciences, Queensland University of Technology, Australia (1996)

Worrest and Caldwell, 1986

R.C. Worrest, M.M. Caldwell (Eds.), Stratospheric Ozone Reduction, Solar Ultraviolet Radiation and Plant Life, Springer-Verlag, Berlin (1986)

Yeloff et al., 2008

D. Yeloff, P. Blokker, P. Boelen, J. Rozema

Is pollen morphology of *Salix polaris* affected by enhanced UV-B irradiation? Results from a field experiment in high arctic tundra

Arctic, Antarctic, and Alpine Research, 40 (4) (2008), pp. 770–774